

Electronic Supplementary Information

Catalytic hairpin assembly-based electrochemical biosensor with tandem signal amplification for sensitive microRNA assay

Lin Cui^{† a}, Jinghua Zhou^{† a}, Xiao-Yun Yang^{† b}, Jing Dong,^c Xiaolei Wang,^{*a} and Chun-yang Zhang^{*a}

^a College of Chemistry, Chemical Engineering and Materials Science, Collaborative Innovation Center of Functionalized Probes for Chemical Imaging in Universities of Shandong, Key Laboratory of Molecular and Nano Probes, Ministry of Education, Shandong Provincial Key Laboratory of Clean Production of Fine Chemicals, Shandong Normal University, Jinan 250014, China

^b Department of Pathology, Affiliated Hospital of Guangdong Medical University, Zhanjiang 524001, China

^c College of Chemistry and Material Science, Shandong Agricultural University, Taian 271018, China.

* Corresponding authors. E-mail: cyzhang@sdnu.edu.cn; wangxl@sdnu.edu.cn; Tel.: +86 0531-86186033. Fax: +86 0531-82615258.

MATERIALS AND METHODS

Materials. Tris (hydroxymethyl) aminomethane (Tris), tris(2-carboxyethyl)phosphine hydrochloride (TCEP) and 6-mercaptohexanol (MCH) were purchased from Sigma-Aldrich Chemical Co. Ltd (USA). Diethylpyrocarbonate (DEPC) was purchased from Sangon Inc. (Shanghai, China). Human breast cancer cell line (MCF-7 cells) was obtained from cell bank of

Chinese academy of sciences (Shanghai, China). All other reagents were of analytical reagent grade. The synthetic oligonucleotides (Table S1) were purchased from Sangon Biological Engineering Technology & Services Co., Ltd. (Shanghai, China) and purified by high-performance liquid chromatography.

Apparatus and characterization. Cyclic voltammograms (CVs) and differential pulse voltammetry (DPV) measurements were carried out on a CHI 660E electrochemical analyzer (CHI, Shanghai, China) at room temperature using a conventional three-electrode system with a modified glassy carbon electrode (GCE) as the working electrode, a platinum wire as the auxiliary electrode, and a saturated calomel electrode (SCE) as the reference electrode. Electrochemical impedance spectroscopic (EIS) analysis was performed with an Zahner workstation (Zahner, Elektrik IM6, German) in 0.1 M KCl containing 5 mM $[\text{Fe}(\text{CN})_6]^{3-}/[\text{Fe}(\text{CN})_6]^{4-}$ over a frequency range from 10 kHz to 0.1 Hz using an alternative voltage with an amplitude of 10 mV.

Preparation of electrochemical biosensor. Prior to the modification, the Au electrode was polished to a mirror-like surface with 1.0, 0.3 and 0.05 μm $\alpha\text{-Al}_2\text{O}_3$ slurry, respectively, followed by successive sonication with ethanol and ultrapure water for 5 min to remove the residual alumina powder. The electrode was then immersed into fresh piranha solution (mixture of concentrated H_2SO_4 and 30% H_2O_2 (3:1 v/v)) for 5 min to remove the adsorbed materials, followed by a thorough rinse with ultrapure water and drying by nitrogen. Subsequently, the electrode was electrochemically cleaned in 0.1 M H_2SO_4 solution by potential scanning between -0.2 and $+1.6$ V at a scan rate of 100 mV s^{-1} until a stable reproducible cyclic voltammogram was obtained. After washing with ultrapure water and drying in a nitrogen stream, the electrode was incubated with 6 μL of 0.2 μM C-DNA which contained 25 μM TCEP (TCEP was used to reduce

the disulfide bonded oligonucleotides) at room temperature for 12 h to make C-DNA immobilize onto the gold electrode surface via gold-sulfur chemistry. Subsequently, 6 μL of 1 mM MCH was dropped on the electrode for 60 min to block the unmodified sites.

Electrochemical detection of miRNA-21. Haipin 1 (H1) and haipin 2 (H2) were annealed by heating at 95 $^{\circ}\text{C}$ for 5 min and then slowly cooled down to room temperature over 3 h. For miRNA-21 assay, 200 nM H1 and 200 nM H2 were mixed with target miRNA at different concentrations in DEPC-treated hybridization solution containing 1 U μL^{-1} RNAase inhibitor and 6 mM MgCl_2 , and incubated for 0.5 h at 37 $^{\circ}\text{C}$. Then the products hybridized with the C-DNA immobilized on the gold electrode for 0.5 h at 37 $^{\circ}\text{C}$. After washing with PBS buffer containing 0.05% Tween-20, 6 μL of 0.1 mg mL^{-1} streptavidin-ALP was dropped onto the above modified electrode at 37 $^{\circ}\text{C}$ for 45 min, followed by washing thoroughly with DEPC-treated PBS (10 mM). The resultant DNA-modified gold electrode was then immersed in the mixture of 200 μM Cu^{2+} and 10 mM AAP (20 mM 3-Morpholinopropanesulfoinc acid (MOPS), 300 mM NaCl, and 2 mM MgCl_2) for 20 min. To measure the in situ formed CuNPs on the gold electrode, the gold electrode was immersed into 0.3 mL of HNO_3 (0.5 M) for 1 h for acid dissolution. Then the solution was added to 4.7 mL of 0.5 M HAc-NaAc buffer (pH 5.0). The resultant mixture was used as the electrolyte for DPASV measurements. The produced Cu^{2+} was electrodeposited on the glassy carbon electrode at -1.0 V for 5 min. Subsequently, DPV was measured from -0.4 to 0.2 V with a scan rate of 50 mV s^{-1} .

Preparation of cell extracts. According to the manufacturer's instructions, the MCF-7 cells were cultured in Dulbecco's modified Eagle's medium (DMEM, Life Technologies, USA) containing 10% fetal bovine serum (FBS, Life Technologies, USA), 100 U/mL penicillin, and 100 U/mL

streptomycin and maintained in a humidified atmosphere with 5% CO₂ at 37 °C. The total RNA was obtained by miRNeasy Mini Kit (Qiagen, German) according to the manufacturer's protocol and its concentration was determined by the NanoDrop 2000c spectrophotometer (Thermo Scientific, Wilmington, DE). The detail procedures are as follows: the cultured cells were treated with trypsin, and then the cell pellet was collected by centrifugation. Subsequently, the miRNA extractor was used to lyse the cells, and the lysed sample was placed at room temperature for 5-10 min, enabling the separation of nucleoproteins from nucleic acids. After adding 0.2 mL of chloroform and shaking vigorously for 30 sec, the sample was placed at room temperature for 3 min. After centrifuging at 12,000 rpm at 4 °C for 10 min, the upper aqueous phase was pipetted into a clean centrifuge tube with the addition of 1.5-fold absolute ethanol. The adsorption column (Spin Column TR) was put into a collection tube, with the solution and translucent fibrous suspension being added to the adsorption column, leaving stand for 1 min, followed by centrifuging at 12,000 rpm for 2 min and pouring off the waste liquid. Then the adsorption column (Spin Column TR) was put back into the collection tube, followed by adding 500 µL of RPE solution, leaving stand for 2 min, centrifuging at 10,000 rpm for 30 sec and discarding the waste liquid. After repeating the above steps for 5 times, the adsorption column (Spin Column TR) was put back into the collection tube and centrifuged at 12,000 rpm for 2 min. Then the adsorption column was placed in a clean 1.5-mL centrifuge tube, followed by adding 30 µL of RNase-free water in the center of adsorption membrane, leaving stand for 2 min, and centrifuging at 12,000 rpm for 2 min. The resultant RNA solution was stored at -70°C prior to measurements.

Gel electrophoresis. To analyze the reaction products, the reaction products were analyzed by 10% nondenaturing polyacrylamide gel electrophoresis (PAGE). PAGE was carried out in 1× TBE

buffer (9 mM Tris-HCl, pH 8.1, 9 mM boric acid, 0.2 mM EDTA) at a 110 V constant voltage for 50 min at room temperature. After electrophoresis, the gel was analyzed by a ChemiDoc™ MP Imaging System (Bio-Rad, Hercules, CA, USA).

SUPPLEMENTARY RESULTS

Electrochemical characterization of different modified electrodes. Cyclic voltammetry (CV) and electrochemical impedance spectroscopy (EIS) were used to monitor each step of GCE modification in 5 mM $[\text{Fe}(\text{CN})_6]^{3-}/[\text{Fe}(\text{CN})_6]^{4-}$ containing 0.1 M KCl. As shown in Fig. S1A, in comparison with the bare GCE (Fig. S1A, curve a), the redox peak current decreased when C-DNA was modified onto the GCE (Fig. S1A, curve b) due to the electrostatic repulsion between $[\text{Fe}(\text{CN})_6]^{3-/4-}$ and the negatively charged phosphate backbones of C-DNA. Moreover, the introduction of nonconductive MCH on the C-DNA/GCE can block the nonspecific site of C-DNA/GCE, leading to the significant decrease of peak current (Fig. S1A, curve c). The subsequent immobilization of target miRNA-21-catalyzed CHA cycle products onto the MCH/C-DNA/GCE modified electrode result in the decrease of redox peak current (Fig. S1A, curve d). This can be explained by the introduction of more negatively charged phosphate backbones onto the electrode surface. The further introduction of nonconductive ALP (Fig. S1A, curve e) onto the H1-H2/MCH/C-DNA/GCE electrode may prevent the transfer of electrons from solution to the electrode surface, resulting in the decrease of redox peak current of CV and the increase of peak-to-peak separation.

The stepwise assembly process of the proposed electrochemical biosensor was further confirmed by EIS. As shown in Fig. S1B, the bare glassy carbon electrode showed a charge transfer impedance (R_{ct}) of 296 Ω (Fig. S1B, curve a). After the C-DNA was assembled on the GCE, the R_{ct} increased slightly to 493 Ω (Fig. S1B, curve b), because the negatively charged phosphate backbone of C-DNA attenuated the electron transfer. With the assembly of short alkanethiol of MCH on the C-DNA/GCE, a large interfacial R_{ct} (2085 Ω) was obtained, because

an insufficient barrier blocked the electron transfer from the solution to the GCE (Fig. S1B, curve c). The hybridization of CHA products with H1-H2 complexes induced a larger resistance of EIS ($R_{ct} = 2855 \Omega$) (Fig. S1B, curve d) due to the strong electrostatic repulsion effect between negatively charged interface and the negatively charged redox probe $[\text{Fe}(\text{CN})_6]^{3-/4-}$. Afterwards, the R_{ct} value increased significantly to (7860 Ω) when the electrode was incubated with ALP (Fig. S1B, curve e). Such increase is caused by the modification of ALP on the electrode surface, and the large volume of ALP may hinder the diffusion of redox probe to the GCE surface.

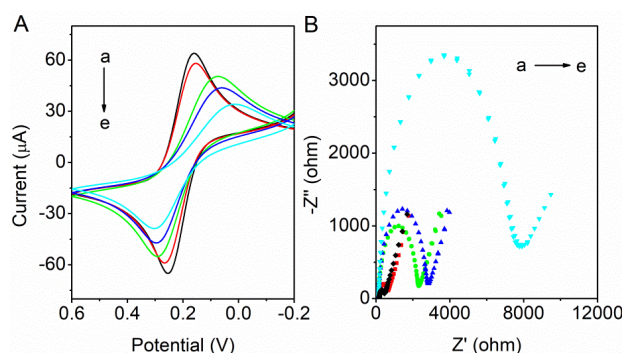


Fig. S1 (A) CV and (B) EIS characterization obtained from different modified GCE in 0.1 M KCl containing 5 mM $[\text{Fe}(\text{CN})_6]^{3-/4-}$ solutions: (a) bare electrode; (b) C-DNA/GCE; (c) MCH/C-DNA/GCE; (d) MiRNA-21/MCH/C-DNA/GCE; (e) ALP/MiRNA-21/MCH/C-DNA/GCE

Quantitation of DNA density on the electrode surface. The amount of C-DNA immobilized on the electrode surface is determined through the measurement of the adsorbed $[\text{Ru}(\text{NH}_3)_6]^{3+}$ by using chronocoulometry on the basis of integrated Cottrell equation¹

$$Q = \frac{2nFAD_0^{1/2}C_0^*}{\pi^{1/2}} t^{1/2} + Q_{dl} + nFA\Gamma_0 \quad (1)$$

Where Q represents the charge $[\text{Ru}(\text{NH}_3)_6]^{3+}$ that diffuses to the electrode surface, Q_{dl} is the capacitive charge, and $nFA\Gamma_0$ represents the charge produced by the adsorbed $[\text{Ru}(\text{NH}_3)_6]^{3+}$. The amount of $[\text{Ru}(\text{NH}_3)_6]^{3+}$ adsorbed to the phosphate backbone of the immobilized DNA (Γ_0), which

can be determined from the difference in intercepts (Δ_{int}) at $t = 0$ in the presence and absence of $[\text{Ru}(\text{NH}_3)_6]^{3+}$, to quantity of the immobilized DNA (Γ_{DNA}) by dividing the number of bases in the single immobilized C-DNA strand ²

$$\Gamma_{\text{DNA}} = \Gamma_0(z/m)N_A \quad (2)$$

Where Γ_{DNA} is the C-DNA surface density, m is the number of bases in the C-DNA, z is the charge of redox molecule, and N_A is Avogadro's number. Based on the chronocoulometric responses of $[\text{Ru}(\text{NH}_3)_6]^{3+}$ (Fig. S2), the surface density of C-DNA on the gold electrode surface is estimated to be 7.005×10^{12} molecules cm^{-2} .

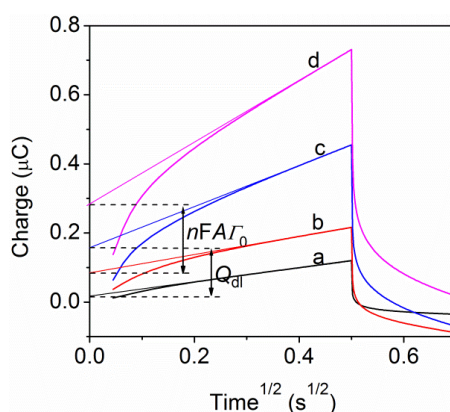


Fig. S2 Chronocoulometric response of MCH (a, c) and C-DNA/MCH (b, d) modified electrodes in the absence (a, b) and presence (c, d) of 50 μM $[\text{Ru}(\text{NH}_3)_6]^{3+}$. Redox charges of $[\text{Ru}(\text{NH}_3)_6]^{3+}$ bound to DNA were obtained from chronocoulometric intercepts at $t = 0$.

Optimization of experimental conditions. To achieve high-performance electrochemical measurements, we optimized the experimental conditions including the concentrations of Cu^{2+} , C-DNA and H1/H2, and incubation time of CHA (Fig. S3). As shown in Fig. S3A, the DPV peak current enhanced with the increase of Cu^{2+} concentration from 50 to 200 μM , and leveled off at 200 μM due to the saturation of the binding sites / active sites. Thus, 200 μM Cu^{2+} was used in the

subsequent researches. The concentration of C-DNA used in the preparation of the biosensor may affect the response of electrochemical biosensor. As shown in Fig. S3B, the peak current enhanced with the increase of C-DNA concentration from 50 to 200 nM, followed by the decrease beyond the concentration of 200 nM due to the steric hindrance at high concentration of C-DNA. Thus, 200 nM C-DNA was used for the preparation of electrochemical biosensor. Fig. S3C shows the effect of the concentrations of H1 or H2 upon the assay performance. The peak current improved with the increasing concentration of H1 / H2 from 0.05 to 1 μ M and reached a maximum at the concentration of 200 nM. Thus, 200 nM H1 / H2 was used in the subsequent researches. The incubation time is an important parameter in electrochemical biosensor. Fig. S3D shows the effect of CHA interaction time upon the electrochemical response. The DPV peak current enhanced with the incubation time from 0 to 30 min and reached the maximum value at 30 min. Hence, the CHA interaction time of 30 min was used in the subsequent researches.

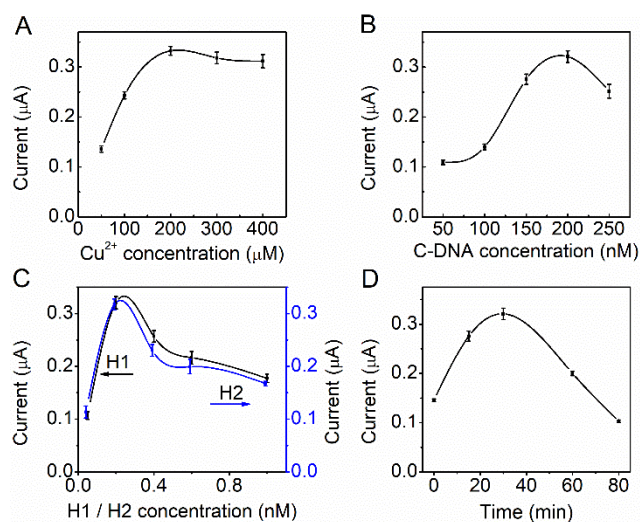


Fig. S3 Effects of Cu^{2+} concentration (A), C-DNA concentration (B), H1 / H2 concentration (C), and CHA reaction time (D) upon the electrochemical response of biosensor. Error bars are standard derivation obtained from three independent experiments.

Stability and reproducibility of the miRNA-21 biosensors. Stability and reproducibility are two important features of electrochemical biosensors for their practical applications. Fig. S4A shows the stability of the electrochemical biosensor triggered by 10 nM target miRNA-21. The DPV responses exhibited little fluctuation with a relative standard deviation (RDS) of 3% and 4.8% after 7 days and 15 days of storage, respectively, indicating the good stability of the proposed electrochemical biosensor.

We investigated the reproducibility of the proposed electrochemical biosensor. The intra-assay (group 1) and inter-assay (group 2) were measured independently under identical conditions for the detection of 10 nM miRNA-21. As shown in Fig. S4B, the relative standard deviation (RSD) for five measurements of 10 nM miRNA-21 using same biosensor under identical conditions is 2.7%, while the RSD for parallel measurements using five freshly prepared modified electrodes with the same process is 3.8%, indicating good reproducibility of the proposed electrochemical biosensor.

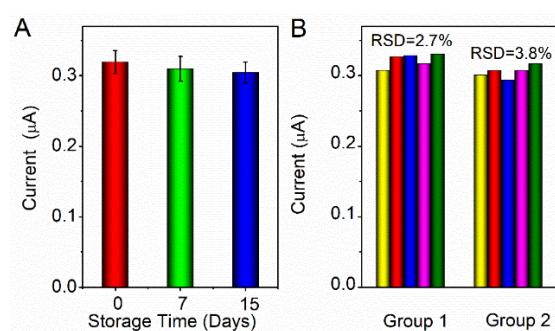


Fig. S4 (A) Long-term storage stability of electrochemical biosensor after storing for different times (0, 7, 15 days). Error bars are standard derivation obtained from three independent experiments. (B) Reproducibility of the electrochemical biosensors for the measurement of 10 nM miRNA-21 under identical conditions. Error bars = RSD (n = 5).

Table S1. Sequence of the oligonucleotides

name	sequence (from 5' to 3')
capture DNA (C-DNA)	HS- <i>TTTTGAGTAGAGTCTGA</i>
hairpin 1 (H1)	biotin- <i>TTTTCAACATC</i> <u><i>CAGTCTGATAAGCTACCATGT</i></u> <i>GTAGATAGCTTATCAGACTCTACTCA</i>
hairpin 2 (H2)	<i>TAAGCTATCTACACATGGTAGCTTATCAGACTCCATG</i> <u><i>TGTAGA</i></u>
miRNA-21	UAG CUU AUC AGA CUG AUG UUG A
single-base mismatch miRNA-21 (M-miRNA-21)	UAG GUU AUC AGA CUG AUG UUG A
miRNA-210	CUG UGC GUG UGA CAG CGG CUG A
miRNA-214	CUG UGC GUG UGA CAG CGG CUG A

The binding regions in C-DNA and Hairpin 1 are shown in italic. The binding regions of Hairpin 1 and Hairpin 2 are shown in underline. The binding regions of Hairpin 1 and miRNA-21 are shown in bold.

Table S2. Comparison of different methods based on CHA for the detection of miRNA-21

detection method	linear range	detection limit	references
fluorescence	4 pM - 40 nM	4 pM	3
fluorescence	0.1 nM - 4 nM	34 pM	4
fluorescence	0.75 - 15 nM	38 pM	5
fluorescence	0.5 - 50 nM	72 pM	6
colorimetric	10 fM - 1 nM	9.2 fM	7
electrochemistry	10 fM - 100pM	4.3 fM	8
electrochemistry	200 pM - 388 nM	100 pM	9
electrochemistry	0.5 pM - 12.5 nM	290 fM	10
electrochemistry	10 fM - 10 nM	1.07 fM	this work

References

1. Y. L. Liu, A. B. Steel, T. M. Herne, M. J. Tarlov, *Anal. Chem.*, 1998, **70**, 4670-4677.
2. J. Zhang, S. Song, L. Zhang, L. Wang, H. Wu, D. Pan, C. Fan, *J. Am. Chem. Soc.*, 2006, **128**, 8575-8580.
3. S. Li, C. Liu, H. Gong, C. Chen, X. Chen, C. Cai, *Talanta*, 2018, **178**, 974-979.
4. H. Fang, N. Xie, M. Ou, J. Huang, W. Li, Q. Wang, J. Liu, X. Yang, K. Wang, *Anal. Chem.*, 2018, **90**, 7164-7170.
5. M. Pan, M. Liang, J. Sun, X. Liu, F. Wang, *Langmuir*, 2018, **34**, 14851-14857.
6. Y. Liu, T. Shen, J. Li, H. Gong, C. Chen, X. Chen, C. Cai, *ACS Sens*, 2017, **2**, 1430-1434.
7. H. Zhang, K. Wang, S. Bu, Z. Li, C. Ju, J. Wan, *Mol. Cell. Probes*, 2018, **38**, 13-18.
8. K. Zhang, Z. Na, Z. Li, H. Wang, H. Shi, L. Qiao, *RSC. Adv.*, 2018, **8**, 16146-16151.
9. J. Mandli, H. Mohammadi, A. Amine, *Bioelectrochemistry*, 2017, **116**, 17-23.

10. Q. Li, F. Zeng, N. Lyu, J. Liang, *Analyst*, 2018, **143**, 2304-2309.